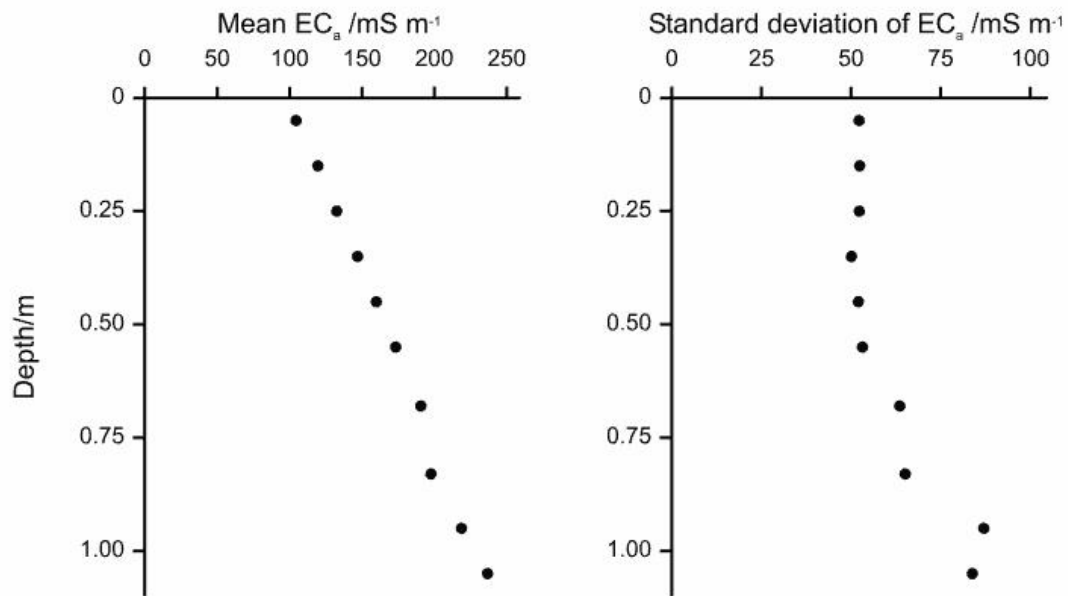
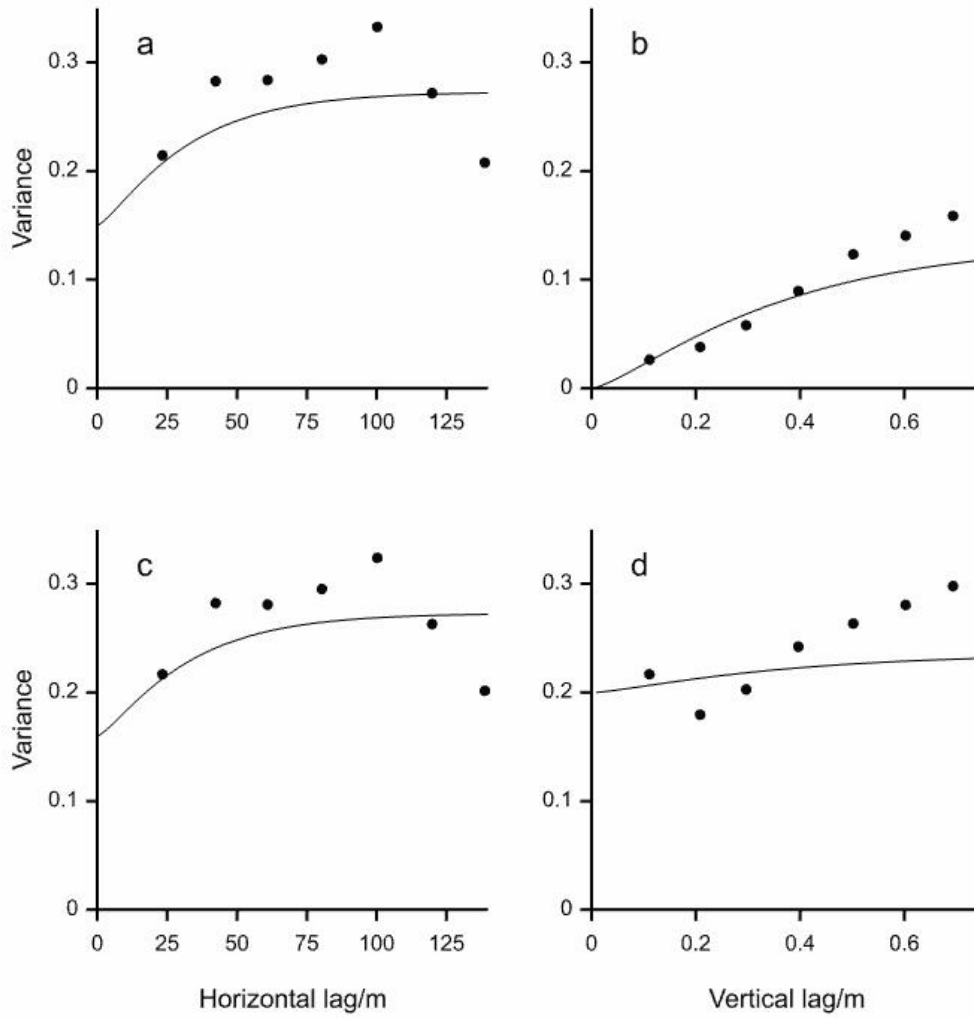


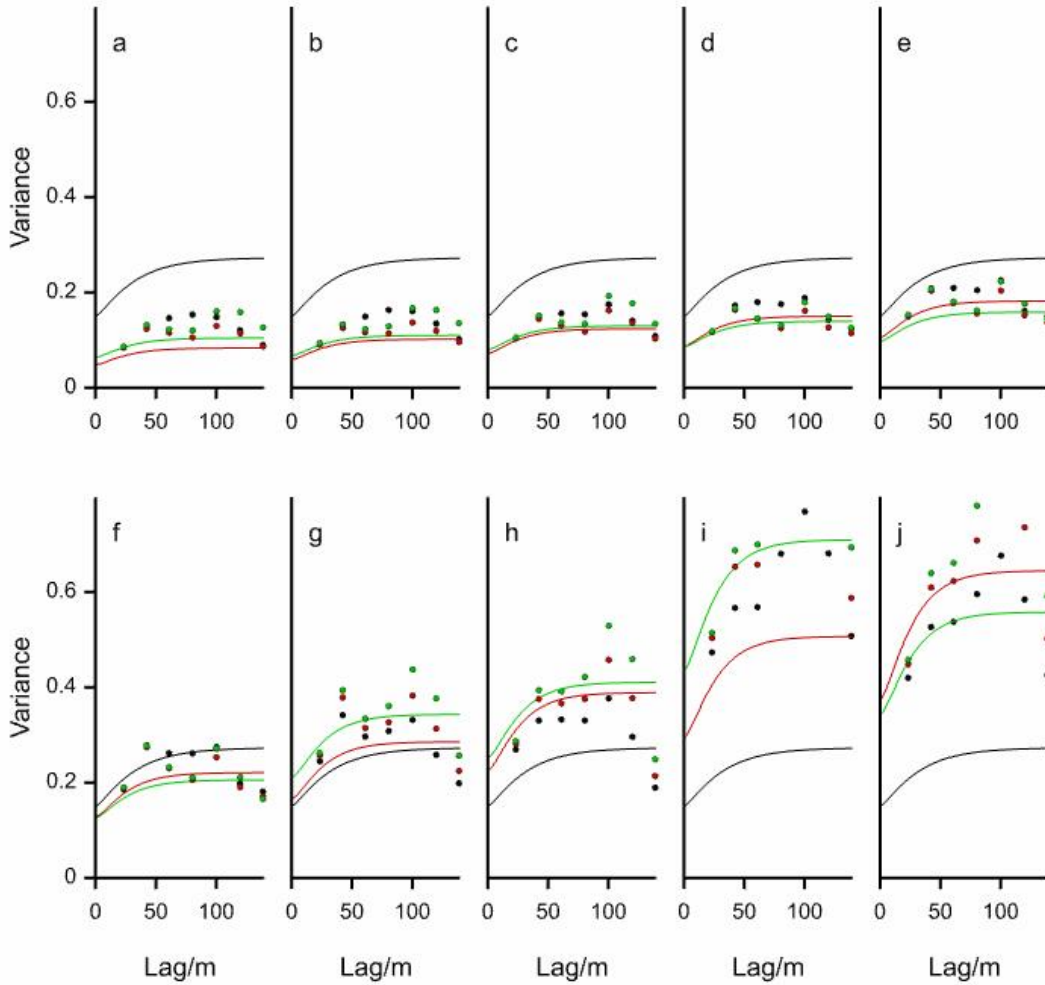
**Fig. 1** Positions of the 56 sampling locations shown by the white circles, the diameters of which are proportional to the mean  $EC_a$  across all ten depths at those points. The grey layers show the horizontal quadratic trend surface fitted to those values.



**Fig. 2** (a) Mean  $EC_a$  plotted against depth; (b) standard deviation of  $EC_a$  plotted against depth.

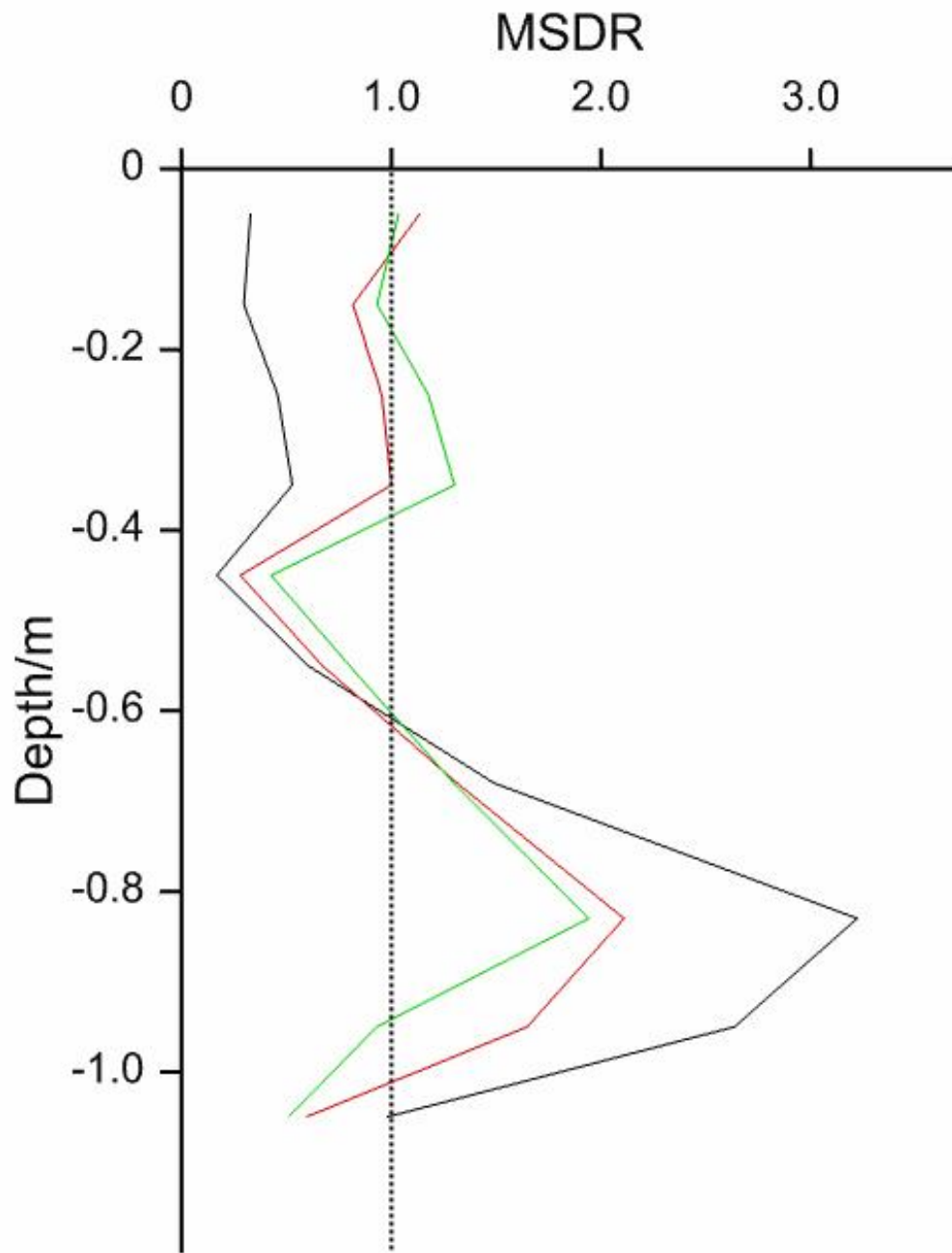


**Fig. 3** Method-of-moments point estimates (black discs) and ML estimated stationary product sum model (curves) of the variogram plotted in the (a) horizontal, (b) vertical, (c) horizontal and displaced by 0.1 m vertically, (d) vertical and displaced by 20 m horizontally dimensions.



**Fig. 4** (a)–(j) Horizontal method of moments point estimates (discs) and ML estimated product sum models (curves) for depths (a) 0.05, (b) 0.15, (c) 0.25, (d) 0.35, (e) 0.45, (f) 0.55, (g) 0.68, (h) 0.83, (i) 0.95 and (j) 1.05 m. Scaling functions are constant (black), cubic (red) and discontinuous (green).

**Fig. 5** MSDR (mean square deviation ratio) against depth for the ML estimated product sum models with constant (black), cubic (red) and discontinuous (green) scaling functions.



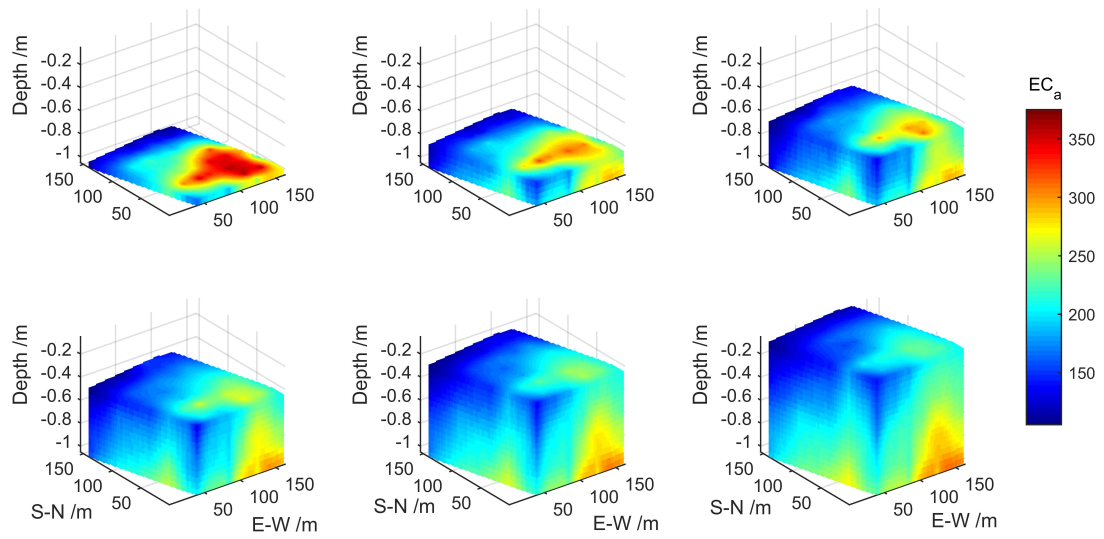


**Fig. 6** Three-dimensional kriged predictions of  $EC_a$  in  $mS\ m^{-1}$ .

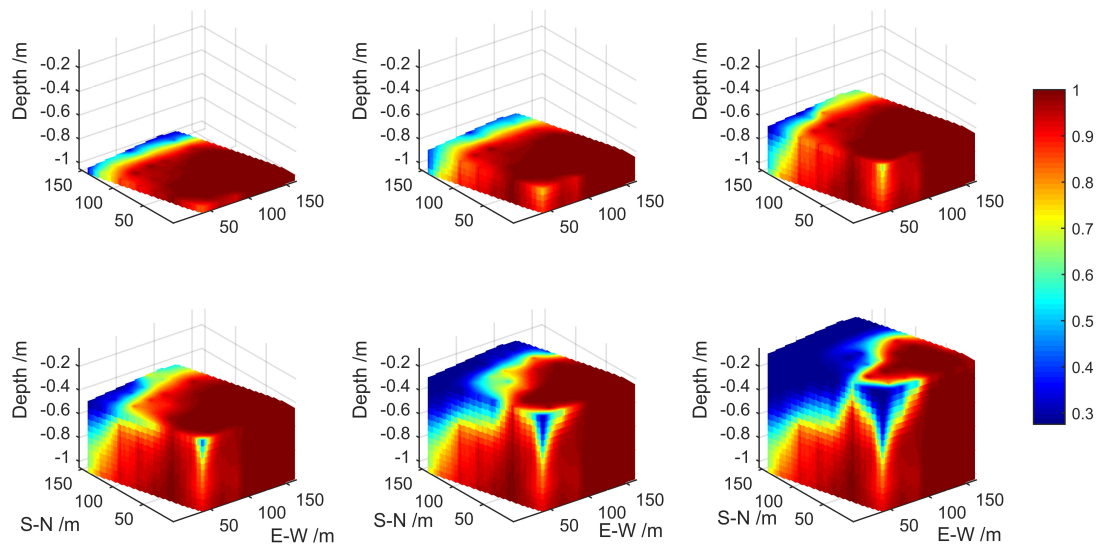


**Fig. 7** The probability that  $EC_a$  exceeds  $123 \text{ mS m}^{-1}$ .